Steady entanglement out of thermal equilibrium

Bruno Bellomo[1, 2, *] and Mauro Antezza[1, 2, †]

[1] *Université Montpellier 2, Laboratoire Charles Coulomb UMR 5221 - F-34095, Montpellier, France*
[2] *CNRS, Laboratoire Charles Coulomb UMR 5221 - F-34095, Montpellier, France*

We study two two-level atomic quantum systems (qubits) placed close to a body held at a temperature different from that of the surrounding walls. While at thermal equilibrium the two-qubit dynamics is characterized by not entangled steady thermal states, we show that absence of thermal equilibrium may bring to the generation of entangled steady states. Remarkably, this entanglement emerges from the two-qubit dissipative dynamic itself, without any further external action on the two qubits, suggesting a new protocol to produce and protect entanglement which is intrinsically robust to environmental effects.

PACS numbers: 03.65.Yz, 03.67.Bg, 03.67.Pp

Introduction.—Entanglement represents one of the key features in quantum mechanics [1], both from a fundamental point of view, due to its connection to non locality [2], and from an applicative one, due to its crucial role in quantum information [3]. Environmental noise [4] induces decoherence effects [5] and is typically responsible for the fragility of entanglement [6]. This represents one of the major obstacles to the concrete realization of quantum technologies related to quantum information processing [1, 3]. A huge effort has been dedicated to the comprehension of the detrimental environmental effects [6–10] and in conceiving suitable approaches to contrast the natural decay of quantum correlations [11]. Several approaches have been theoretically proposed and experimentally tested. They include reservoir engineering [11], feedback methods [12], distillation protocols [13], decoherence free-subspaces [14], non-Markovian effects [7], weak measurements [15], quantum Zeno effect [16], dynamical decoupling [17] and reservoir monitoring [18].

Here, we introduce a new direct procedure to protect entanglement realized by bringing the environment of a two-qubit system out of thermal equilibrium. Physical systems consisting of two qubits in a common environment in absence [19] or presence [20] of matter have been largely investigated at thermal equilibrium, pointing out the creation of entanglement due to the field mediated interaction, which however typically washes off asymptotically. Efforts have been also done considering two qubits interacting with independent ideal blackbody reservoirs at different temperatures [21]. New possibilities emerging in realistic systems out of thermal equilibrium have been recently pointed out in different contexts ranging form heat transfer [22], to Casimir-Lifshits forces [23–25] and atomic dynamics [26].

In this Letter, we consider a system made by two qubits interacting with the complex electromagnetic field out of thermal equilibrium resulting from the presence of bodies at different temperature and whose scattering properties play a key role. We will show that this particular environmental noise has two remarkable effects: it *contrasts* the usual dechoerence between the qubits, and it *generates* steady entangled states. This production and protection of entanglement is obtained without any further external actions on the two qubits, such as the use of lasers or complex procedures involving measurements on the qubits or on the environment, and without the need of initializing the total system in a given configuration.

Physical system and model.—We consider two qubits $q = 1, 2$, whose ground $|g\rangle_q$ and excited $|e\rangle_q$ internal levels are separated by the frequency $\omega = \omega_e^1 - \omega_g^1 = \omega_e^2 - \omega_g^2$, interacting with a complex environment consisting in a stationary out of thermal equilibrium electromagnetic field. This is the result of the field emitted by a body of arbitrary geometry and dielectric permittivity, held at the temperature T_{M}, and of the field emitted by far surrounding walls held at temperature T_{W}, eventually reflected and transmitted by the body (see Fig. 1 when the body is a slab). The walls have an irregular shape and are distant enough from the qubits such that the field they would produce at the qubits position (in the absence of the body) would be a blackbody radiation independent from the walls composition and geometry [23]. The total Hamiltonian has the form $H = H_S + H_E + H_I$, where $H_S = \sum_q \sum_{n=g,e} \hbar\omega_n^q \sigma_{nn}^q$, being $\sigma_{mn}^q = |m\rangle_{qq}\langle n|$, is the free two-qubit Hamiltonian and H_E the free environmental Hamiltonian. The interaction between the qubits and the environment in the multipolar coupling and in dipole approximation is described by $H_I = -\sum_q \mathbf{D}_q \cdot \mathbf{E}(\mathbf{R}_q)$

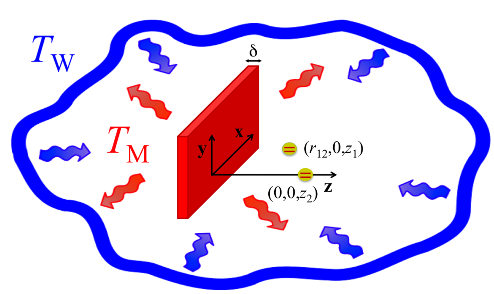

FIG. 1: (color online). Two qubits close to a slab at temperature T_{M} different from the temperature of the surrounding walls, T_{W}.

[27], where $\mathbf{D}_q$ is the electric-dipole operator of qubit q (being ${}_q\langle g|\mathbf{D}_q|e\rangle_q = \mathbf{d}^q$), and $\mathbf{E}(\mathbf{R}_q)$ is the electric field at the position $\mathbf{R}_q$ of qubit q.

Master equation.—The starting point to study the two-qubit dynamics is the von Neumann equation for the total density matrix, which in the interaction picture is $\dot{\rho}_{\rm tot}(t) = -\frac{i}{\hbar}[H_I(t), \rho_{\rm tot}(t)]$. By tracing over the environmental degrees of freedom, after the Born, Markov and rotating wave approximations, the master equation for the reduced two-qubit density matrix becomes [28, 29]

$$\begin{aligned}\frac{d}{dt}\rho = &-\frac{i}{\hbar}[H_S+\delta_S,\rho] - i\sum_{q\neq q'}\Lambda^{qq'}(\omega)[\sigma_{ge}^{q\,\dagger}\sigma_{ge}^{q'},\rho]\\ &+\sum_{q,q'}\Gamma^{qq'}(\omega)\Big(\sigma_{ge}^{q'}\rho\sigma_{ge}^{q\,\dagger} - \frac{1}{2}\{\sigma_{ge}^{q\,\dagger}(\omega)\sigma_{ge}^{q'}(\omega),\rho\}\Big)\\ &+\sum_{q,q'}\Gamma^{qq'}(-\omega)\Big(\sigma_{ge}^{q'\,\dagger}\rho\sigma_{ge}^{q}(\omega) - \frac{1}{2}\{\sigma_{ge}^{q}\sigma_{ge}^{q'\,\dagger},\rho\}\Big),\end{aligned} \tag{1}$$

where δ_S is an operator related to the level frequency shifts, not playing any role in the following. Function $\Lambda^{qq'}(\omega)$ represents temperature independent induced coherent (dipole-dipole) interaction between the qubits, while $\Gamma^{qq'}(\pm\omega)$ are individual ($q = q'$) and common field mediated collective ($q \neq q'$) qubit transition rates, related to both quantum and thermal fluctuations of the electromagnetic field at the qubits positions.

To discuss the properties of master equation (1), we will use two standard different basis: the decoupled bases $\{|1\rangle \equiv |gg\rangle, |2\rangle \equiv |eg\rangle, |3\rangle \equiv |ge\rangle, |4\rangle \equiv |ee\rangle\}$, and the coupled bases $\{|{\rm G}\rangle \equiv |1\rangle, |{\rm A}\rangle \equiv (|2\rangle - |3\rangle)/\sqrt{2}, |{\rm S}\rangle \equiv (|2\rangle + |3\rangle)/\sqrt{2}, |{\rm E}\rangle \equiv |4\rangle\}$, where the collective antisymmetrical and symmetrical states $|{\rm A}\rangle$ and $|{\rm S}\rangle$ are combinations of the decoupled states $|2\rangle$ and $|3\rangle$.

X states and concurrence.—In the decoupled basis, master equation (1) implies that the dynamics of the elements along the two main diagonals of the two-qubit density matrix (forming an X-structure) is independent from that of the remaining ones. Then, an initial state with an X-structure maintains its form in time. Moreover, terms outside the two main diagonals, are washed off asymptotically. Bell, Werner and Bell diagonal states belong to the class of X states [30], which arise in a wide variety of physical situations and are experimentally achievable [31]. In the following we will deal with X states.

We quantify the two-qubit entanglement by means of the concurrence $C(t)$ ($C = 0$ for separable states, $C = 1$ for maximally entangled states) [32]. For X states, using $\rho_{ij} = \langle i|\rho|j\rangle$, it takes the simple form [33]

$$\begin{aligned}C(t) &= 2\max\{0, K_1(t), K_2(t)\},\\ K_1(t) &= |\rho_{23}(t)| - \sqrt{\rho_{11}(t)\rho_{44}(t)},\\ K_2(t) &= |\rho_{14}(t)| - \sqrt{\rho_{22}(t)\rho_{33}(t)}.\end{aligned} \tag{2}$$

Eq. (1) induces an exponential decay for $\rho_{14}(t)$, so that in the steady state only $K_1(t)$ could lead to $C(\infty) > 0$.

Thermal equilibrium.—For $T_{\rm W} = T_{\rm M}$ master equation (1) describes the qubits thermalization towards the diagonal thermal equilibrium state [34]

$$\begin{pmatrix}\rho_{11}(\infty)\\ \rho_{22}(\infty)\\ \rho_{33}(\infty)\\ \rho_{44}(\infty)\end{pmatrix}_{\rm eq} = \frac{1}{Z_{\rm eq}}\begin{pmatrix}[1+n(\omega,T)]^2\\ n(\omega,T)[1+n(\omega,T)]\\ n(\omega,T)[1+n(\omega,T)]\\ n(\omega,T)^2\end{pmatrix}, \tag{3}$$

where $Z_{\rm eq} = [1 + 2\ n(\omega,T)]^2$ and $n(\omega,T) = (e^{\frac{\hbar\omega}{k_{\rm B}T}} - 1)^{-1}$. This state is universal, it depends only on the ratio $\hbar\omega/k_{\rm B}T$, remaining insensible to all system details. Being $|\rho_{23}(\infty)| = 0$, $K_1(\infty)$ is always negative, resulting in *not entangled steady states*. In terms of the density matrix in the coupled bases, using $\rho_{\rm X} \equiv \rho_{\rm XX} = \langle {\rm X}|\rho|{\rm X}\rangle$,

$$|\rho_{23}| = \frac{1}{2}\sqrt{(\rho_{\rm S}-\rho_{\rm A})^2 + (\rho_{\rm AS}-\rho_{\rm AS}^*)^2}, \tag{4}$$

which is equal to zero in the steady state since $\rho_{\rm AS}(\infty) = 0$ and $\rho_{\rm S}(\infty) = \rho_{\rm A}(\infty)$. The latter identity has not to be valid out of thermal equilibrium, allowing $K_1(\infty) > 0$ hence producing steady entanglement.

Out of thermal equilibrium.—For $T_{\rm W} \neq T_{\rm M}$, the analysis of Eqs. (1-2) is much more rich and delicate. The Γ and Λ functions depend on the correlation functions of the electromagnetic field, which at thermal equilibrium can be directly evaluated exploiting the fluctuation-dissipation theorem (FDT). Out equilibrium, the FTD is not valid in general. Nevertheless, we assume that the radiation emission by the body and the walls has the same characteristics it would have at thermal equilibrium at the source temperature [23, 25]. This allows to compute the correlation functions by indirectly using the FDT, as recently used to study the dynamics of a single atom [26]. The transition rates in Eq. (1) can be set under the form

$$\begin{aligned}\Gamma^{qq'}(\omega) =& \sqrt{\Gamma_0^q(\omega)\Gamma_0^{q'}(\omega)}\Big\{[1+n(\omega,T_{\rm W})]\alpha_{\rm W}^{qq'}(\omega)\\ &+[1+n(\omega,T_{\rm M})]\alpha_{\rm M}^{qq'}(\omega)\Big\}\\ \Gamma^{qq'}(-\omega) =& \sqrt{\Gamma_0^q(\omega)\Gamma_0^{q'}(\omega)}\Big\{n(\omega,T_{\rm W})\alpha_{\rm W}^{qq'}(\omega)^*\\ &+n(\omega,T_{\rm M})]\alpha_{\rm M}^{qq'}(\omega)^*\Big\},\end{aligned} \tag{5}$$

where $\alpha_{\rm W}^{qq'}(\omega) = \sum_{i,i'}[\tilde{\mathbf{d}}^q]_i^*[\tilde{\mathbf{d}}^{q'}]_{i'}[\alpha_{\rm W}^{qq'}(\omega)]_{ii'}$, $\alpha_{\rm M}^{qq'}(\omega) = \sum_{i,i'}[\tilde{\mathbf{d}}^q]_i^*[\tilde{\mathbf{d}}^{q'}]_{i'}[\alpha_{\rm M}^{qq'}(\omega)]_{ii'}$, being $[\tilde{\mathbf{d}}^q]_i = [\mathbf{d}^q]_i/|\mathbf{d}^q|$, and $\Gamma_0^q(\omega) = |\mathbf{d}^q|^2\omega^3/3\hbar\pi\epsilon_0 c^3$ is the vacuum spontaneous-emission rate of qubit q. $[\alpha_{\rm M}^{qq'}(\omega)]_{ii'}$ and $[\alpha_{\rm W}^{qq'}(\omega)]_{ii'}$ are temperature independent functions, which depend on all the other system parameters (qubits positions and frequency, dielectric and geometric properties of the body) and can be expressed in terms of the reflection and transmission operators associated to the body (see appendix).

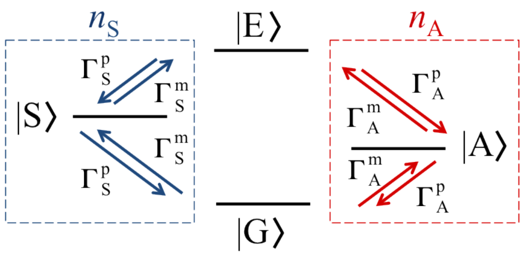

FIG. 2: (color online). Scheme of the rate equations of Eq. (7): $\Gamma^{p}_{\mathrm{S(A)}} = \Gamma_{\mathrm{S(A)}}(1+n_{\mathrm{S(A)}})$, $\Gamma^{m}_{\mathrm{S(A)}} = \Gamma_{\mathrm{S(A)}}\, n_{\mathrm{S(A)}}$.

The $\Lambda^{qq'}(\omega)$ function of Eq. (1) can be expressed as

$$\Lambda^{qq'}(\omega) = \frac{\sqrt{\Gamma_0^{q}(\omega)\Gamma_0^{q'}(\omega)}}{\omega^3} \times \mathcal{P}\int_{-\infty}^{+\infty} \frac{\omega'^3 d\omega'}{2\pi}\frac{\alpha_{\mathrm{W}}^{qq'}(\omega') + \alpha_{\mathrm{M}}^{qq'}(\omega')}{\omega-\omega'}, \tag{6}$$

and calculated using the Kramers-Kronig relations (see Appendix).

Analytical investigation.—To illustrate the new qualitative and quantitative behaviour of the entanglement out of thermal equilibrium, we first consider an instructive case allowing a direct interpretation. Let us consider $\Gamma^{11}(\pm\omega) = \Gamma^{22}(\pm\omega) \equiv \Gamma(\pm\omega)$ and $\Gamma^{12(21)}(\pm\omega) \in \mathbb{R}$. These conditions are verified for identical qubits ($\mathbf{d}^1 = \mathbf{d}^2 \equiv \mathbf{d}$) in equivalent positions with respect to the body (in the case the body is a slab, $z_1 = z_2$) and with $\mathbf{d}$ real and directed or along the z axis or along the $x-y$ plane. In this case, master equation (1) implies in the coupled basis a set of *rate equations* for the populations, decoupled from the other density matrix elements:

$$\begin{aligned}
\dot\rho_{\mathrm{G}} =& \Gamma_{\mathrm{A}}(1+n_{\mathrm{A}})\rho_{\mathrm{A}} + \Gamma_{\mathrm{S}}(1+n_{\mathrm{S}})\rho_{\mathrm{S}} \\
&- (\Gamma_{\mathrm{A}}\, n_{\mathrm{A}} + \Gamma_{\mathrm{S}}\, n_{\mathrm{S}})\rho_{\mathrm{G}} +, \\
\dot\rho_{\mathrm{A}} =& \Gamma_{\mathrm{A}}\, n_{\mathrm{A}}\rho_{\mathrm{G}} + \Gamma_{\mathrm{A}}(1+n_{\mathrm{A}})\rho_{\mathrm{E}} - \Gamma_{\mathrm{A}}(1+2n_{\mathrm{A}})\rho_{\mathrm{A}}, \\
\dot\rho_{\mathrm{S}} =& \Gamma_{\mathrm{S}}\, n_{\mathrm{S}}\rho_{\mathrm{G}} + \Gamma_{\mathrm{S}}(1+n_{\mathrm{S}})\rho_{\mathrm{E}} - \Gamma_{\mathrm{S}}(1+2n_{\mathrm{S}})\rho_{\mathrm{S}}, \\
\dot\rho_{\mathrm{E}} =& \Gamma_{\mathrm{A}}\, n_{\mathrm{A}}\rho_{\mathrm{A}} + \Gamma_{\mathrm{S}}\, n_{\mathrm{S}}\rho_{\mathrm{S}} \\
&- [\Gamma_{\mathrm{A}}(1+2n_{\mathrm{A}}) + \Gamma_{\mathrm{S}}(1+2n_{\mathrm{S}})]\rho_{\mathrm{E}}.
\end{aligned} \tag{7}$$

Here the derivates are with respect to $\Gamma_0(\omega)t$ [$\Gamma_0(\omega) \equiv \Gamma_0^{(1)}(\omega) = \Gamma_0^{(2)}(\omega)$], and we introduced the symmetric and anti-symmetric rates and the effective number of photons

$$\begin{aligned}
\Gamma_{\mathrm{A}} =& \alpha_{\mathrm{W}}(\omega) - \alpha_{\mathrm{W}}^{12}(\omega) + \alpha_{\mathrm{M}}(\omega) - \alpha_{\mathrm{M}}^{12}(\omega) \\
\Gamma_{\mathrm{S}} =& \alpha_{\mathrm{W}}(\omega) + \alpha_{\mathrm{W}}^{12}(\omega) + \alpha_{\mathrm{M}}(\omega) + \alpha_{\mathrm{M}}^{12}(\omega) \\
n_{\mathrm{A}} =& \frac{1}{\Gamma_{\mathrm{A}}}\Big\{\big[\alpha_{\mathrm{W}}(\omega) - \alpha_{\mathrm{W}}^{12}(\omega)\big]\, n(\omega, T_{\mathrm{W}}) \\
&+ \big[\alpha_{\mathrm{M}}(\omega) - \alpha_{\mathrm{M}}^{12}(\omega)\big]\, n(\omega, T_{\mathrm{M}})\Big\} \\
n_{\mathrm{S}} =& \frac{1}{\Gamma_{\mathrm{S}}}\Big\{\big[\alpha_{\mathrm{W}}(\omega) + \alpha_{\mathrm{W}}^{12}(\omega)\big]\, n(\omega, T_{\mathrm{W}}) \\
&+ \big[\alpha_{\mathrm{M}}(\omega) + \alpha_{\mathrm{M}}^{12}(\omega)\big]\, n(\omega, T_{\mathrm{M}})\Big\},
\end{aligned} \tag{8}$$

being $\alpha_{\mathrm{W(M)}}(\omega) \equiv \alpha_{\mathrm{W(M)}}^{11}(\omega) = \alpha_{\mathrm{W(M)}}^{22}(\omega)$. We remark that function Λ does not enter in the rate equations (7), which are depicted in Fig. 2. To each decay channel from $|\mathrm{E}\rangle$ to $|\mathrm{G}\rangle$, passing respectively trough $|\mathrm{S}\rangle$ and $|\mathrm{A}\rangle$, one can associate an effective number of photons $n_{\mathrm{S(A)}}$ confined between $n(\omega, T_{\mathrm{W}})$ and $n(\omega, T_{\mathrm{M}})$, which is equivalent to associate an effective temperature $T_{\mathrm{S(A)}}$ confined between T_{W} and T_{M} [26]. It is possible to show that while the coherences along the second diagonal decay exponentially to zero, the stationary solution of Eq. (7) is

$$\begin{pmatrix} \rho_{\mathrm{G}}(\infty) \\ \rho_{\mathrm{A}}(\infty) \\ \rho_{\mathrm{S}}(\infty) \\ \rho_{\mathrm{E}}(\infty) \end{pmatrix}_{\mathrm{neq}} = \frac{1}{Z_{\mathrm{neq}}} \begin{pmatrix} (1+n_{\mathrm{A}})^2(1+2n_{\mathrm{S}})\Gamma_{\mathrm{A}} + (1+2n_{\mathrm{A}})(1+n_{\mathrm{S}})^2\Gamma_{\mathrm{S}} \\ n_{\mathrm{A}}(1+n_{\mathrm{A}})(1+2n_{\mathrm{S}})\Gamma_{\mathrm{A}} + [n_{\mathrm{A}}(1+2n_{\mathrm{S}}) + n_{\mathrm{S}}^2(1+2n_{\mathrm{A}})]\Gamma_{\mathrm{S}} \\ n_{\mathrm{S}}(1+n_{\mathrm{S}})(1+2n_{\mathrm{A}})\Gamma_{\mathrm{S}} + [n_{\mathrm{S}}(1+2n_{\mathrm{A}}) + n_{\mathrm{A}}^2(1+2n_{\mathrm{S}})]\Gamma_{\mathrm{A}} \\ n_{\mathrm{A}}^2(1+2n_{\mathrm{S}})\Gamma_{\mathrm{A}} + (1+2n_{\mathrm{A}})n_{\mathrm{S}}^2\Gamma_{\mathrm{S}} \end{pmatrix}, \tag{9}$$

where Z_{neq} is the sum of the elements of the vector on the right side of the above equation. Equation (9), which reduces to (3) for $T_{\mathrm{W}} = T_{\mathrm{M}}$, shows that out of equilibrium it is possible that $\rho_{\mathrm{S}}(\infty) \neq \rho_{\mathrm{A}}(\infty)$, and implies $|\rho_{23}(\infty)| = |n_{\mathrm{S}} - n_{\mathrm{A}}|(\Gamma_{\mathrm{S}} + \Gamma_{\mathrm{A}})/2Z_{\mathrm{neq}}$ trough Eq. (4). This leads to the possibility to have $K_1(\infty) > 0$ in Eq. (2), corresponding to stationary entanglement. Using Eq. (9) in Eq. (2), we obtain for the steady concurrence $C(\infty) = 2\ \max\{0, K_1(\infty)\}$, with

$$\begin{aligned}
K_1(\infty) = \frac{2}{Z_{\mathrm{neq}}}\Big[&|n_{\mathrm{S}} - n_{\mathrm{A}}|(\Gamma_{\mathrm{S}} + \Gamma_{\mathrm{A}})/2 \\
&- \sqrt{(1+n_{\mathrm{A}})^2(1+2n_{\mathrm{S}})\Gamma_{\mathrm{A}} + (1+2n_{\mathrm{A}})(1+n_{\mathrm{S}})^2\Gamma_{\mathrm{S}}} \\
&\times \sqrt{n_{\mathrm{A}}^2(1+2n_{\mathrm{S}})\Gamma_{\mathrm{A}} + (1+2n_{\mathrm{A}})n_{\mathrm{S}}^2\Gamma_{\mathrm{S}}}\Big],
\end{aligned} \tag{10}$$

which tends to zero at thermal equilibrium when $n_{\mathrm{S}} = n_{\mathrm{A}}$. Simplifying Γ_{S}, $C(\infty)$ becomes function of only

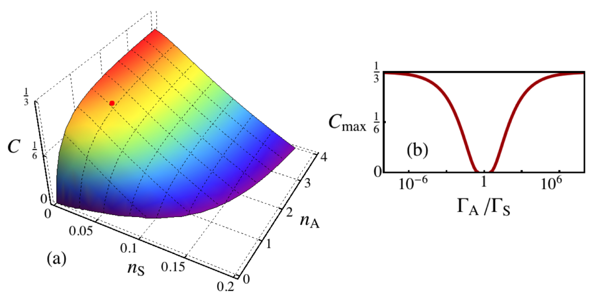

FIG. 3: (color online). Part (a): steady concurrence $[C = C(\infty)]$ vs $n_{\rm S}$ and $n_{\rm A}$ for a fixed value $\Gamma_{\rm A}/\Gamma_{\rm S} \approx 2.8 \times 10^{-4}$. Part (b): maximum of concurrence, $C_{\rm max}$ as function of $\Gamma_{\rm A}/\Gamma_{\rm S}$.

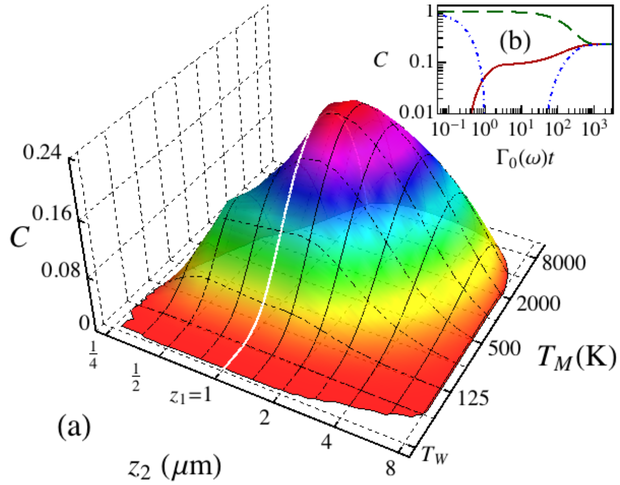

FIG. 4: (color online). Part (a): steady concurrence $[C = C(\infty)]$ vs z_2 and $T_{\rm M}$. Here $z_1 = 1\mu$m, $r_{12} = 0.25\mu$m (the qubits are distant $[r_{12}^2 + (z_1 - z_2)^2]^{1/2}$), $T_{\rm W} = 30$ K, $\delta = 0.01\mu$m, and $\omega = 0.3\omega_r$. Part (b): dynamics of concurrence as a function of $\Gamma_0(\omega)t$ for three different initial conditions, the antisymmetric (green dashed line), the symmetric (blue dotdashed line) and the thermal state at 30 K (red solid line).

$\Gamma_{\rm A}/\Gamma_{\rm S}$, $n_{\rm S}$ and $n_{\rm A}$. We discuss this dependence in Fig. 3 (a), where $C(\infty)$ is depicted as a function of $n_{\rm S}$ and $n_{\rm A}$ for $\Gamma_{\rm A}/\Gamma_{\rm S} \approx 2.8 \times 10^{-4}$. It is shown that large values of steady concurrence are obtained when the number of photons associated to the two decay channels (see Fig.2), that is their effective temperatures, are enough distant between them. This physically corresponds to largely populate the antisymmetric state with respect to the symmetric one [see Eqs. (9) and (4)]. By increasing too much $n_{\rm A}$ at fixed $n_{\rm S}$, the steady entanglement starts to decrease (not shown in the figure). Part (b) shows that the maximum value of $C(\infty)$ reachable by varying $n_{\rm S}$ and $n_{\rm A}$ at a fixed value of $\Gamma_{\rm A}/\Gamma_{\rm S}$ is 1/3, obtainable in the two cases $\Gamma_{\rm A}/\Gamma_{\rm S} \to 0$ or $\Gamma_{\rm S}/\Gamma_{\rm A} \to 0$. We remark that up to now our findings do not rely on the specific choice of body's geometry or dielectric properties.

Numerical investigation.—In order to discuss the properties of $C(\infty)$ besides the case studied above, we solve Eq. (1) for the case where the body close to the two qubits is a slab of thickness δ, as depicted in Fig. 1. In this case $\alpha_{\rm M}^{qq'}$ and $\alpha_{\rm W}^{qq'}$ of Eq. (5) can be expressed as integrals over propagative and evanescent sectors (see Appendix). We also choose a SiC slab, describing its dielectric permittivity with a Drude-Lorentz model, with a resonance at $\omega_r = 1.495 \times 10^{14}\,\text{rad}\,\text{s}^{-1}$ and a surface phonon-polariton resonance at $\omega_p = 1.787 \times 10^{14}\,\text{rad}\,\text{s}^{-1}$. Hence, relevant length and temperature scales are $c/\omega_r \simeq 2\mu$m and $\hbar\omega_r/k_B \simeq 1140$ K. In Fig. 4 (a) we plot concurrence of Eq. (2) as a function of z_2 and $T_{\rm M}$ in the case of two identical qubits having electric dipole perpendicular to the slab, for fixed values of $z_1 = 1\mu$m and $T_{\rm W} = 30$ K. The plot evidences a large zone in the space of the parameters corresponding to the generation of steady entangled states. The maximum value of $C(\infty)$, obtained for $z_1 \neq z_2 = 1.28$ and $T_{\rm M} \approx 1300$ K, is ≈ 0.224. The characteristic time to reach this entangled steady state is $\simeq 10^3[\Gamma_0(\omega)]^{-1}$ [see part (b)]. The white line corresponds to the case $z_2 = z_1$ and hence can be described by Eq. (10). The maximum along this curve, obtained for $T_{\rm M} \approx 1200$ K, corresponds to the red point in Fig. 3 (a), being $n_{\rm A} \approx 1.53$ ($T_{\rm A} \approx 680$ K) and $n_{\rm S} \approx 0.02$ ($T_{\rm S} \approx 90$ K). The relevant difference between $T_{\rm S}$ and $T_{\rm A}$ is responsible of the high value of concurrence, ≈ 0.217 (see also Fig. 3). However, by further increasing $T_{\rm M}$ (comporting an increase of the difference between $T_{\rm S}$ and $T_{\rm A}$) the concurrence decreases. In Fig. 4 (b), by using the parameters corresponding to the maximum of Fig. 4(a), we show the time evolution of concurrence for three different initial states: the maximally entangled antisymmetric and symmetric states, and the not entangled thermal state at $T = 30$ K. We note how the protection of entanglement and its steady production, respectively, are independent on the initial two-qubit state. A systematic study shows also that by increasing the slab thickness δ, or the value of r_{12}, or moving the atomic frequency ω towards the slab resonances, or changing the two qubits electric dipole orientations steady entanglement typically reduces. We observe that even a small amount of mixed state entanglement, here produced, could be then distilled into a pure entangled state [35].

Conclusions.— We investigated the dynamics of two qubits interacting with a common stationary field out of thermal equilibrium. We predicted the occurrence of steady entangled states not depending on the initial two-qubit state, consisting then in a creation and/or protection of entanglement according to the nature of the initial configuration. For a relevant class of parameters we derived an analytical expression for concurrence, and explained the entanglement production in terms of rate equations driven by two different effective temperatures associated to the two decay channels governing the passage from the two-qubit excited state to the ground state. We numerically studied the case where the body close to

the qubits is a slab, finding concurrence up to $\approx 1/4$ for conservative parameters's values. While at thermal equilibrium the entanglement decays to zero faster if the temperature is increased, this new strategy to create and/or protect entanglement can be realized, quite counterintuitively, starting from a thermal equilibrium configuration and *increasing* only one of the two temperatures of the system. To further increase the amount of steady entanglement, systematic studies exploiting different body's geometries are envisaged.

Appendix: α functions

The expressions for the functions $[\alpha^{qq'}_{\mathrm{W}}(\omega)]_{ii'}$ and $[\alpha^{qq'}_{\mathrm{M}}(\omega)]_{ii'}$ appearing in Eq. (5), in the case the body forming part of the environment of the two qubits has an arbitrary geometry and dielectric function, are [the two qubits are placed in $(\mathbf{r}_1, z_1)$ and $(\mathbf{r}_2, z_2)$, where $\mathbf{r}_1$ and $\mathbf{r}_2$ are vectors in the xy plane]

$$\begin{aligned}
[\alpha^{qq'}_{\mathrm{W}}(\omega)]_{ii'} &= \frac{3\pi c}{2\omega}\sum_{p,p'}\int\frac{d^2\mathbf{k}}{(2\pi)^2}\int\frac{d^2\mathbf{k}'}{(2\pi)^2}e^{i(\mathbf{k}\cdot\mathbf{r}_q-\mathbf{k}'\cdot\mathbf{r}_{q'})}\langle p,\mathbf{k}|\Big\{e^{i(k_z z_q-k_z'^* z_{q'})}[\hat{\boldsymbol{\epsilon}}^+_p(\mathbf{k},\omega)]_i[\hat{\boldsymbol{\epsilon}}^+_{p'}(\mathbf{k}',\omega)]^*_{i'}\\
&\times\Big(\mathcal{T}\mathcal{P}^{(\mathrm{pw})}_{-1}\mathcal{T}^\dagger+\mathcal{R}\mathcal{P}^{(\mathrm{pw})}_{-1}\mathcal{R}^\dagger\Big)+e^{i(k_z z_q+k_z'^* z_{q'})}[\hat{\boldsymbol{\epsilon}}^+_p(\mathbf{k},\omega)]_i[\hat{\boldsymbol{\epsilon}}^-_{p'}(\mathbf{k}',\omega)]^*_{i'}\mathcal{R}\mathcal{P}^{(\mathrm{pw})}_{-1}\\
&+e^{-i(k_z z_q+k_z'^* z_{q'})}[\hat{\boldsymbol{\epsilon}}^-_p(\mathbf{k},\omega)]_i[\hat{\boldsymbol{\epsilon}}^+_{p'}(\mathbf{k}',\omega)]^*_{i'}\mathcal{P}^{(\mathrm{pw})}_{-1}\mathcal{R}^\dagger+e^{-i(k_z z_q-k_z'^* z_{q'})}[\hat{\boldsymbol{\epsilon}}^-_p(\mathbf{k},\omega)]_i[\hat{\boldsymbol{\epsilon}}^-_{p'}(\mathbf{k}',\omega)]^*_{i'}\mathcal{P}^{(\mathrm{pw})}_{-1}\Big\}|p',\mathbf{k}'\rangle
\end{aligned}\tag{11}$$

$$\begin{aligned}
[\alpha^{qq'}_{\mathrm{M}}(\omega)]_{ii'} &= \frac{3\pi c}{2\omega}\sum_{p,p'}\int\frac{d^2\mathbf{k}}{(2\pi)^2}\int\frac{d^2\mathbf{k}'}{(2\pi)^2}e^{i(\mathbf{k}\cdot\mathbf{r}_q-\mathbf{k}'\cdot\mathbf{r}_{q'})}\langle p,\mathbf{k}|\Big\{e^{i(k_z z_q-k_z'^* z_{q'})}[\hat{\boldsymbol{\epsilon}}^+_p(\mathbf{k},\omega)]_i[\hat{\boldsymbol{\epsilon}}^+_{p'}(\mathbf{k}',\omega)]^*_{i'}\\
&\times\Big[\Big(\mathcal{P}^{(\mathrm{pw})}_{-1}-\mathcal{R}\mathcal{P}^{(\mathrm{pw})}_{-1}\mathcal{R}^\dagger+\mathcal{R}\mathcal{P}^{(\mathrm{ew})}_{-1}-\mathcal{P}^{(\mathrm{ew})}_{-1}\mathcal{R}^\dagger-\mathcal{T}\mathcal{P}^{(\mathrm{pw})}_{-1}\mathcal{T}^\dagger\Big)\Big\}|p',\mathbf{k}'\rangle,
\end{aligned}$$

where the operators $\mathcal{R}$ and $\mathcal{T}$ are the standard reflection and transmission scattering operators, explicitly defined for example in [25], associated in this case to the right side of the body. They connect any outgoing (reflected or transmitted) mode of the field to the entire set of incoming modes. In the two previous equations, each mode of the field is identified by the frequency ω, the transverse wave vector $\mathbf{k} = (k_x, k_y)$, the polarization index p (taking the values $p = 1, 2$ corresponding to TE and TM polarizations respectively), and the direction or propagation $\phi = \pm 1$ (shorthand notation $\phi = \pm$) along the z axis. In this approach, the total wavevector takes the form $\mathbf{K}^\phi = (\mathbf{k}, \phi k_z)$, where the z component of the wavevector k_z is a dependent variable given by $k_z = \sqrt{\frac{\omega^2}{c^2} - k^2}$, where $k = |\mathbf{k}|$. For the polarization vectors appearing in Eq. (11) we adopt the following standard definitions

$$\begin{aligned}
\hat{\boldsymbol{\epsilon}}^\phi_{\mathrm{TE}}(\mathbf{k},\omega) &= \hat{\mathbf{z}}\times\hat{\mathbf{k}} = \frac{1}{k}(-k_y\hat{\mathbf{x}}+k_x\hat{\mathbf{y}}),\\
\hat{\boldsymbol{\epsilon}}^\phi_{\mathrm{TM}}(\mathbf{k},\omega) &= \frac{c}{\omega}\hat{\boldsymbol{\epsilon}}^\phi_{\mathrm{TE}}(\mathbf{k},\omega)\times\mathbf{K}^\phi = \frac{c}{\omega}(-k\hat{\mathbf{z}}+\phi k_z\hat{\mathbf{k}}),
\end{aligned}\tag{12}$$

where $\hat{\mathbf{x}}$, $\hat{\mathbf{y}}$ and $\hat{\mathbf{z}}$ are the unit vectors along the three axes and $\hat{\mathbf{k}} = \mathbf{k}/k$. In Eq. (11) we have also used

$$\langle p,\mathbf{k}|\mathcal{P}^{(\mathrm{pw/ew})}_n|p',\mathbf{k}'\rangle = k_z^n\langle p,\mathbf{k}|\Pi^{(\mathrm{pw/ew})}|p',\mathbf{k}'\rangle,\tag{13}$$

$\Pi^{(\mathrm{pw})}$ and $\Pi^{(\mathrm{ew})}$ being the projectors on the propagative ($ck < \omega$, corresponding to a real k_z) and evanescent ($ck > \omega$, corresponding to a purely imaginary k_z) sectors respectively.

In the case when the body is a slab, we have at disposition simple expressions for $\mathcal{R}$ and $\mathcal{T}$. As a result of the translational invariance of a planar slab with respect to the xy plane, its reflection and transmission operators, $\mathcal{R}$ and $\mathcal{T}$, are diagonal and given by

$$\begin{aligned}
\langle p,\mathbf{k}|\mathcal{R}|p',\mathbf{k}'\rangle &= (2\pi)^2\delta(\mathbf{k}-\mathbf{k}')\delta_{pp'}\rho_p(\mathbf{k},\omega),\\
\langle p,\mathbf{k}|\mathcal{T}|p',\mathbf{k}'\rangle &= (2\pi)^2\delta(\mathbf{k}-\mathbf{k}')\delta_{pp'}\tau_p(\mathbf{k},\omega),
\end{aligned}\tag{14}$$

where the Fresnel reflection and transmission coefficients modified by the finite thickness δ are equal to

$$\begin{aligned}
\rho_p(\mathbf{k},\omega) &= r_p(\mathbf{k},\omega)\frac{1-e^{2ik_{zm}\delta}}{1-r_p^2(\mathbf{k},\omega)e^{2ik_{zm}\delta}},\\
\tau_p(\mathbf{k},\omega) &= \frac{t_p(\mathbf{k},\omega)\bar{t}_p(\mathbf{k},\omega)e^{i(k_{zm}-k_z)\delta}}{1-r_p^2(\mathbf{k},\omega)e^{2ik_{zm}\delta}}.
\end{aligned}\tag{15}$$

In these definitions we have introduced the z component of the $\mathbf{K}$ vector inside the medium,

$$k_{zm} = \sqrt{\varepsilon(\omega)\frac{\omega^2}{c^2}-\mathbf{k}^2},\tag{16}$$

$\varepsilon(\omega)$ being the dielectric permittivity of the slab, the ordinary vacuum-medium Fresnel reflection coefficients

$$r_{\mathrm{TE}}=\frac{k_z-k_{zm}}{k_z+k_{zm}},\qquad r_{\mathrm{TM}}=\frac{\varepsilon(\omega)k_z-k_{zm}}{\varepsilon(\omega)k_z+k_{zm}},\tag{17}$$

as well as both the vacuum-medium (noted with t) and medium-vacuum (noted with $\bar{t}$) transmission coefficients

$$\begin{aligned}t_{\mathrm{TE}}&=\frac{2k_z}{k_z+k_{zm}}, & t_{\mathrm{TM}}&=\frac{2\sqrt{\varepsilon(\omega)}k_z}{\varepsilon(\omega)k_z+k_{zm}},\\ \bar{t}_{\mathrm{TE}}&=\frac{2k_{zm}}{k_z+k_{zm}}, & \bar{t}_{\mathrm{TM}}&=\frac{2\sqrt{\varepsilon(\omega)}k_{zm}}{\varepsilon(\omega)k_z+k_{zm}}.\end{aligned}\tag{18}$$

Using Eq. (14), Eq. (11) reduces in the simpler case when the body is a slab to

$$\begin{aligned}[\alpha_{\mathrm{W}}^{qq'}(\omega)]_{ii'}&=\frac{[A^{qq'}(\omega)]^*_{ii'}+[B^{qq'}(\omega)]_{ii'}+2[C^{qq'}(\omega)]_{ii'}}{2}\\ [\alpha_{\mathrm{M}}^{qq'}(\omega)]_{ii'}&=\frac{[A^{qq'}(\omega)]_{ii'}-[B^{qq'}(\omega)]_{ii'}+2[D^{qq'}(\omega)]_{ii'}}{2},\end{aligned}\tag{19}$$

where we have introduced the integral matrices

$$\begin{aligned}[A^{qq'}(\omega)]_{ii'}=&\frac{3c}{4\omega}\sum_p\int_0^{\frac{\omega}{c}}\frac{k\,dk}{k_z}e^{ik_z(z_q-z_{q'})}[N_p^{qq'}(k,\omega)]^{++}_{ii'}\\ [B^{qq'}(\omega)]_{ii'}=&\frac{3c}{4\omega}\sum_p\int_0^{\frac{\omega}{c}}\frac{k\,dk}{k_z}e^{ik_z(z_q-z_{q'})}[N_p^{qq'}(k,\omega)]^{++}_{ii'}\\ &\times\big(|\rho_p(k,\omega)|^2+|\tau_p(k,\omega)|^2\big),\\ [C^{qq'}(\omega)]_{ii'}=&\frac{3c}{4\omega}\sum_p\int_0^{\frac{\omega}{c}}\frac{k\,dk}{k_z}\,\mathrm{Re}\big\{e^{ik_z(z_q+z_{q'})}\\ &\times[N_p^{qq'}(k,\omega)]^{+-}_{ii'}\,\rho_p(k,\omega)\big\},\\ [D^{qq'}(\omega)]_{ii'}=&\frac{3c}{4\omega}\sum_p\int_{\frac{\omega}{c}}^{+\infty}\frac{k\,dk}{\mathrm{Im}(k_z)}e^{-\mathrm{Im}(k_z)(z_q+z_{q'})}\\ &\times[N_p^{qq'}(k,\omega)]^{++}_{ii'}\,\mathrm{Im}[\rho_p(k,\omega)],\end{aligned}\tag{20}$$

where [we choose the x axis along the vector $\mathbf{r}_q-\mathbf{r}_{q'}$ whose coordinates in the plane xy are then $(r_{qq'},0)$]

$$[N_1^{qq'}(k,\omega)]^{\phi\phi'}_{ii'}=\begin{pmatrix}\frac{2}{kr_{qq'}}J_1(kr_{qq'}) & 0 & 0\\ 0 & \frac{2}{kr_{qq'}}J_1(kr_{qq'})-2J_2(kr_{qq'}) & 0\\ 0 & 0 & 0\end{pmatrix},$$

$$[N_2^{qq'}(k,\omega)]^{\phi\phi'}_{ii'}=\begin{pmatrix}\frac{2\phi\phi'c^2|k_z^2|}{kr_{qq'}\omega^2}\Big[J_1(kr_{qq'})-kr_{qq'}J_2(kr_{qq'})\Big] & 0 & -i\phi\frac{2c^2kk_z}{\omega^2}J_1(kr_{qq'})\\ 0 & \frac{2\phi\phi'c^2|k_z^2|}{kr_{qq'}\omega^2}J_1(kr_{qq'}) & 0\\ -i\phi'\frac{2c^2kk_z^*}{\omega^2}J_1(kr_{qq'}) & 0 & \frac{2c^2k^2}{\omega^2}J_0(kr_{qq'})\end{pmatrix},$$

where i runs over the rows and i' over the columns and where $J_n(x)$ is Bessel function of the n kind.

Concerning $\Lambda^{qq'}(\omega)$ of Eq. (6), we can exploit the connection between α functions and the imaginary part of the Green function of the system,

$$\mathrm{Im}\,G_{ii'}(\mathbf{R}_q,\mathbf{R}_{q'},\omega)=\frac{\omega^3}{3\pi\epsilon_0c^3}\frac{[\alpha_{\mathrm{W}}^{qq'}(\omega)]_{ii'}+[\alpha_{\mathrm{M}}^{qq'}(\omega)]_{ii'}}{2},\tag{21}$$

where i and i' refer to the cartesian components of the field and $G_{ii'}(\mathbf{R}_q,\mathbf{R}_{q'},\omega)$ is the ii' component of the Green function of the system, solution of the differential equation (for two arbitrary $\mathbf{R}$ and $\mathbf{R}'$)

$$\Big[\nabla_{\mathbf{R}}\times\nabla_{\mathbf{R}}-\frac{\omega^2}{c^2}\epsilon(\omega,\mathbf{R})\Big]\mathbb{G}(\mathbf{R},\mathbf{R}',\omega)=\frac{\omega^2}{\epsilon_0c^2}\,\mathbb{I}\,\delta(\mathbf{R}-\mathbf{R}')\tag{22}$$

being $\mathbb{I}$ the identity dyad and $\epsilon(\omega,\mathbf{R})$ the dielectric function. Using Eq. (21), Eq. (6) becomes

$$\begin{aligned}\Lambda^{qq'}(\omega)=&-\frac{1}{\hbar}\sum_{i,i'}[\mathbf{d}^q]^*_i[\mathbf{d}^{q'}]_{i'}\\ &\times\mathcal{P}\int_{-\infty}^{+\infty}\frac{d\omega'}{\pi}\frac{\mathrm{Im}\,G_{ii'}(\mathbf{R}_q,\mathbf{R}_{q'},\omega')}{\omega'-\omega}\\ =&-\frac{1}{\hbar}\sum_{i,i'}[\mathbf{d}^q]^*_i[\mathbf{d}^{q'}]_{i'}\,\mathrm{Re}\,G_{ii'}(\mathbf{R}_q,\mathbf{R}_{q'},\omega),\end{aligned}\tag{23}$$

where Kramers-Kronig relations connecting real and imaginary parts of the green function have been used to compute the principal value of the integral.

In the case of a slab, it can be shown that previous equation reduces to

$$\Lambda^{qq'}(\omega) =\Lambda_0^{qq'}(\omega) + \sqrt{\Gamma_0^{q}(\omega)\Gamma_0^{q'}(\omega)}\sum_{i,i'}[\tilde{\mathbf{d}}^{q}]_i^*[\tilde{\mathbf{d}}^{q'}]_{i'} \times\big([C_2^{qq'}(\omega)]_{ii'} - [D_2^{qq'}(\omega)]_{ii'}\big), \tag{24}$$

where $[\tilde{\mathbf{d}}^{q}]_i = [\mathbf{d}^{q}]_i/|\mathbf{d}^{q}|$ and $\Lambda_0^{qq'}(\omega)$ is the free term remaining in absence of matter around the two qubits

$$\begin{aligned}\Lambda_0^{qq'}(\omega) =& -\frac{3}{4}\sqrt{\Gamma_0^{q}(\omega)\Gamma_0^{q'}(\omega)}\Big\{\big[\tilde{\mathbf{d}}^{q\,*}\cdot\tilde{\mathbf{d}}^{q'} - (\tilde{\mathbf{d}}^{q\,*}\cdot\tilde{\mathbf{r}})\\ &\times(\tilde{\mathbf{d}}^{q'}\cdot\tilde{\mathbf{r}})\big]\Big[\frac{(\tilde{r}^2-1)\cos\tilde{r}-\tilde{r}\sin\tilde{r}}{\tilde{r}^3}\Big]\\ &+2(\tilde{\mathbf{d}}^{q^*}\cdot\tilde{\mathbf{r}})\,(\tilde{\mathbf{d}}^{q'}\cdot\tilde{\mathbf{r}})\Big[\frac{\cos\tilde{r}+\tilde{r}\sin\tilde{r}}{\tilde{r}^3}\Big]\Big\},\end{aligned} \tag{25}$$

being $\tilde{r} = |\tilde{\mathbf{r}}| = |\mathbf{r}_q - \mathbf{r}_{q'}|\omega/c$, and where we have introduced the new integral matrices

$$\begin{aligned}[C_2^{qq'}(\omega)]_{ii'} =&\frac{3c}{8\omega}\sum_p\int_0^{\frac{\omega}{c}}\frac{k\,dk}{k_z}\,\mathrm{Im}\big(e^{ik_z(z_q+z_{q'})}\\ &\times[N_p^{qq'}(k,\omega)]_{ii'}^{+-}\,\rho_p(k,\omega)\big),\\ [D_2^{qq'}(\omega)]_{ii'} =&\frac{3c}{8\omega}\sum_p\int_{\frac{\omega}{c}}^{+\infty}\frac{k\,dk}{\mathrm{Im}(k_z)}e^{-\,\mathrm{Im}(k_z)(z_q+z_{q'})}\\ &\times[N_p^{qq'}(k,\omega)]_{ii'}^{++}\,\mathrm{Re}(\rho_p(k,\omega)).\end{aligned} \tag{26}$$

Acknowledgments.—Authors thank R. Messina for useful discussions and acknowledge financial support from the Julian Schwinger Foundation.

* Electronic address: bruno.bellomo@univ-montp2.fr
† Electronic address: mauro.antezza@univ-montp2.fr

[1] R. Horodecki *et al.*, Rev. Mod. Phys. **81**, 865 (2009).
[2] A. Einstein, B. Podolsky, and N. Rosen, Phys. Rev. **47**, 777 (1935); J. F. Clauser, M. A. Horne, A. Shimony, and R. A. Holt, Phys. Rev. Lett. **23**, 880 (1969).
[3] M. A. Nielsen and I. L. Chuang, *Quantum Computation and Quantum Information* (Cambridge Univ. Press, 2000).
[4] H.-P. Breuer and F. Petruccione, *The Theory of Open Quantum Systems* (Oxford Univ. Press, New York, 2002).
[5] W. H. Zurek, Rev. Mod. Phys. **75**, 715 (2003).
[6] T. Yu and J. H. Eberly, Phys. Rev. Lett. **93**, 140404 (2004).
[7] B. Bellomo, R. Lo Franco, and G. Compagno, Phys. Rev. Lett. **99**, 160502 (2007); Phys. Rev. A **77**, 032342 (2008).
[8] R. Lo Franco, B. Bellomo, E. Andersson, and G. Compagno, Phys. Rev. A **85**, 032318 (2012).
[9] M. P. Almeida *et al.*, Science **316**, 579582 (2007).
[10] J. S. Xu *et al.*, Phys. Rev. Lett. **104**, 100502 (2010).
[11] F. Verstraete, M. M. Wolf, and J. I. Cirac, Nat. Phys. **5**, 633 (2009).
[12] R. N. Stevenson, J. J. Hope, and A. R. R. Carvalho, Phys. Rev. A **84**, 022332 (2011).
[13] P. G., Kwiat, S. Barraza-Lopez, A. Stefanov, and N. Gisin, Nature **409**, 10141017 (2001).
[14] D. A. Lidar, I. L. Chuang, and K. B. Whaley, Phys. Rev. Lett. **81**, 2594 (1998).
[15] Y.-S. Kim, J.-C. Lee, O. Kwon, and Y.-H. Kim, Nat. Phys. **8**, 117 (2012).
[16] S. Maniscalco, F. Francica, R. L. Zaffino, N. Lo Gullo, and F. Plastina, Phys. Rev. Lett. **100**, 090503 (2008).
[17] L. Viola, E. Knill, and S. Lloyd, Phys. Rev. Lett. **82**, 2417 (1999).
[18] A. R. R. Carvalho and M. F. Santos, New J. Phys. **13**, 013010 (2011).
[19] D. Braun, Phys. Rev. Lett. **89**, 277901 (2002); F. Benatti, R. Floreanini, and M. Piani, Phys. Rev. Lett. **91**, 070402 (2003); Z. Ficek and R. Tanaś, Phys. Rev. A **77**, 054301 (2008).
[20] A. Gonzalez-Tudela *et al.*, Phys. Rev. Lett. **106**, 020501 (2011); J. Xu, M. Al-Amri, Y. Yang, S. Y. Zhu, and M. S. Zubairy, Phys. Rev. A **84**, 032334 (2011).
[21] S. Camalet, Eur. Phys. J. B. **84**, 467 (2011).
[22] K. Joulain *et al.*, Surf. Sci. Rep. **57**, 59 (2005); R. Messina, M. Antezza, and P. Ben-Abdallah, Phys. Rev. Lett. **109**, 244302 (2012).
[23] M. Antezza, L. P. Pitaevskii, and S. Stringari, Phys. Rev. Lett. **95**, 113202 (2005); M. Antezza, J. Phys. A: Math. Gen. **39**, 6117 (2006); J. M. Obrecht *et al.*, Phys. Rev. Lett. **98**, 063201 (2007); M. Antezza, L. P. Pitaevskii, S. Stringari, and V. B. Svetovoy, Phys. Rev. A **77**, 022901 (2008).
[24] G. Bimonte, Phys. Rev. A **80**, 042102 (2009); M. Krüger, T. Emig, and M. Kardar, Phys. Rev. Lett. **106**, 210404 (2011).
[25] R. Messina and M. Antezza, Europhys. Lett. **95**, 61002 (2011); Phys. Rev. A **84**, 042102 (2011).
[26] B. Bellomo, R. Messina, and M. Antezza, Europhys. Lett. **100**, 20006 (2012); B. Bellomo, R. Messina, D. Felbacq, and M. Antezza, Phys. Rev. A **87**, 012101 (2013).
[27] C. Cohen-Tannoudji, J. Dupont-Roc, and G. Grynberg, *Photons and Atoms: Introduction to Quantum Electrodynamics* (Wiley, 1997).
[28] G. S. Agarwal, in *Quantum Statistical Theories of Spontaneous Emission and their Relation to other Approaches, edited by G. Höhler*, Springer Tracts in Modern Physics Vol. 70 (Springer-Verlag, Berlin, 1974).
[29] Z. Ficek and S. Swain, *Quantum Interference and Coherence: Theory and Experiments*, (Springer, New York, 2005).
[30] B. Bellomo, R. Lo Franco and G. Compagno, Adv. Sci. Lett. **2**, 459 (2009).
[31] L. Di Carlo *et al.*, Nature **460** 240 (2009);
[32] W. K. Wootters Phys. Rev. Lett. **80**, 2245 (1998).
[33] T. Yu and J. H. Eberly, Quantum Information and Computation **7**, 459 (2007).
[34] The thermal state is not reached asymptotically if $\Gamma^{ii}(\pm\omega) = \Gamma^{ij}(\pm\omega)$. In this case, both at and out thermal equilibrium, the steady state depends upon the initial state.
[35] M. Horodecki, P. Horodecki, and R. Horodecki, Phys. Rev. Lett. **78**, 574 (1997).